

Second Born model for two-electron atomic ionization by fast charged particle impact

A. S. Kheifets

Research School of Physical Sciences,

*The Australian National University, Canberra ACT 0200, Australia**

(Dated: September 9, 2003)

Abstract

We develop a theoretical model to describe simultaneous ionization-excitation and double ionization of a two-electron atomic shell (i.e. He $1s^2$) by a fast charged particle impact. The model accounts for the projectile-target interaction to the second order whereas the interaction of the two target electrons in continuum is treated non-perturbatively by the convergent close-coupling (CCC) method. In the second order term, all intermediate states of the target between two subsequent interactions with the projectile are weighted equally with an average energy denominator (the so-called closure approximation) and only the dipole interaction of the projectile with the target is included. The model is suited to describe two-electron ionization processes with large projectile velocity, small momentum transfer and small to intermediate energy of the ejected electrons. The model is applied to ionization-excitation and double ionization of He by electron and proton impact in kinematics of recent experiments.

*Electronic address: A.Kheifets@anu.edu.au; URL: <http://rsphysse.anu.edu.au/~ask107>

I. INTRODUCTION

Two-electron ionization processes caused by charged particle impact such as ionization with simultaneous excitation and double ionization are strongly dependent on many-electron correlations [1]. However, unlike the two-electron single-photon ionization processes, which are driven entirely by correlations, charged particle impact can cause a two-electron transition in the absence of correlations simply by repeated interaction of the projectile with the target. This competition of the electron correlations in the target and a complicated dynamics of the reaction makes it difficult to interpret particle-induced two-electron ionization. However, there exists a case when the correlations and dynamics can be clearly disentangled. Indeed, if the projectile is fast, its interaction with the target can be treated perturbatively (the so-called low perturbation regime) by employing a Born series expansion. This effectively reduces the problem of four interacting charged particles to a three-body Coulomb problem which is encountered in the two-electron ionization caused by photon impact. The latter problem can be treated by employing either an asymptotically exact three-body Coulomb wave function or a close-coupling expansion to account for interaction of the two target electrons in continuum.

It is believed that in the Born series on the projectile-target interaction, only the two lowest terms (the so-called first and second Born terms) contribute significantly to the two-electron ionization [2]. The first Born term has been investigated in great detail and the benchmark results had been established for the electron-impact ionization-excitation of He to the $n = 2$ state [3, 4]. There is also a good agreement between different close-coupling theories for the second Born contribution as far as ionization-excitation is concerned [5, 6]. However, there is a broad variation of the first and second Born results for the double ionization by electron impact. There is no agreement in the first Born model between the convergent close-coupling method and the calculations based on the asymptotically exact three-body Coulomb final state, popularly known as BBK [7]. The latter method exhibits a very strong, sometime counterintuitive, dependence on the accuracy of the ground state, when an inferior ground state gives a better agreement with experiment on the absolute scale [8, 9]. The second Born results are even more erratic as various BBK calculations do not agree between themselves. For instance, Choubisa et al. [10] reported recently rather significant contribution of the second Born term at the electron incident energy of 5.5 keV.

At the same time, Mkhater and Cappello [11] found a very weak contribution of this term at exactly the same kinematics. There had been an attempt to treat the full four-body problem non-perturbatively by employing either an asymptotically exact four-body Coulomb wave function [12] or by a Faddeev-type expansion [13]. But these results are either at variance with reported first and second Born calculations or explore the kinematics where Born calculations had not been reported.

In this paper, we present a new second Born model based on the CCC description of the two-electron final state. In our earlier work, we applied the CCC formalism to electron impact ionization with excitation and double ionization (the so-called (e,3e) reaction) in the first Born regime. The model was used to describe the two-electron ionization at a very large projectile energy of 5.5 keV [3, 14]. In subsequent (e,3e) experiments, the energy of the projectile was lowered to 2 keV [15, 16] and some deviations from the first Born regime became obvious. In particular, the symmetry of the angular distribution of the two ejected electrons with respect to the momentum transfer direction was broken, especially in the angular region of the recoil peak, and when momentum transfer was small $q < 1$ [15]. In the impulsive regime $q > 1$, deviation from the first Born regime was not so obvious [16]. Recent (e,3e) experiments with very low projectile energy of 0.5 keV [17, 18] clearly demonstrated very strong deviation from the first Born regime. To interpret these experiments, we extended our first Born implementation of the CCC method to include the second Born term in the projectile-target interaction. The combined first and second Born results were found in a much better agreement with experiment [18]. Limited space of a rapid communication did not allow us to present all the computational details and results of numerous tests we performed to assure the accuracy of our model. In the present paper we give these missing details. In addition, we present an extensive set of (e,3e) calculations in comparison with experimental data of Lahmam-Bennani et al. [8, 17] and Dorn et al. [16, 18]. We also perform calculations for double ionization of He by proton impact and compare our results with the latest experimental data of Fischer et al. [19]. This experiment demonstrated a clear difference between the electron and proton impact double ionization at the same projectile velocity which can only be attributed to the second (and higher) Born effects.

The structure of the paper is as follows. In Section II we give the basic formalism of the second Born implementation of the CCC method. In section III A we test our model

by calculating electron impact ionization of He leading to the $n = 2$ excited state. We compare our results with available experimental data [20, 21] as well as the earlier second Born calculations [5, 6]. As our model is restricted to dipole interaction in the second Born term, we also compare our results with analogous data obtained by the R -matrix method with pseudostates (RMPS) with all the multipoles included in the second Born term and the dipole contribution only [22]. In Section III B we give our (e,3e) results for various electron impact energies. In Section III C we present the proton impact double ionization data. We conclude by outlining further directions of this project.

II. FORMALISM

A. First and second Born amplitudes with a plane wave projectile

Formal derivation of the Born series expansion is given by Walters [2]. Here we only outline briefly details of the formalism specific to the CCC method. For simplicity, we assume the projectile to be electron. Extension to an arbitrary charged projectile is trivial.

We use a continuum wave normalization $\langle \mathbf{k} | \mathbf{k}' \rangle = \delta(\mathbf{k} - \mathbf{k}')$ with an asymptotics at infinity $|\mathbf{k}\rangle \approx (2\pi)^{-3/2} e^{i\mathbf{k}\mathbf{r}}$. With this normalization the incident flux is $j = k_0/(2\pi)^3$ and the cross-section of a two-electron ionization process caused by particle impact is written as

$$\sigma_f^{(e,2e)} = (2\pi)^4 \frac{k_1 k_2}{k_0} \sum_{m_f} \left| F_f^{B1}(\mathbf{q}, \mathbf{k}_2) + F_f^{B2}(\mathbf{k}_0, \mathbf{k}_1, \mathbf{k}_2) \right|^2. \quad (1)$$

Here we assign indices 0, 1 and 2 to the projectile before and after collision, and the ejected electron, respectively. Index f refers to the remaining target electron, either in the bound state (ionization-excitation) or continuum (double ionization). In the latter case the energy of the ejected electron is matched by positive energy pseudostate $\epsilon_f = k_3^2/2$.

We treat a fast projectile as a plane wave and write the first Born amplitude as

$$F^{B1} = \langle \mathbf{k}_1 \Psi_f(\mathbf{k}_2) | U | \mathbf{k}_0 \Psi_0 \rangle = \frac{4\pi}{q^2} \frac{1}{(2\pi)^3} \langle \Psi_f(\mathbf{k}_2) | e^{i\mathbf{q}\mathbf{r}} + e^{i\mathbf{q}\mathbf{r}'} - 2 | \Psi_0 \rangle \quad (2)$$

Here we applied the Bethe transformation to the projectile-target interaction

$$U = -\frac{Z}{\mathbf{r}_0} + \frac{1}{|\mathbf{r}_0 - \mathbf{r}|} + \frac{1}{|\mathbf{r}_0 - \mathbf{r}'|}, \quad (3)$$

where \mathbf{r}_0 , \mathbf{r} and \mathbf{r}' are coordinates of the projectile and the two target electrons, respectively. In the following we consider the two-electron ionization of the He atom and set $Z = 2$ in the

nucleus term. The momentum transfer from the projectile to the target $\mathbf{q} = \mathbf{k}_0 - \mathbf{k}_1$. By commuting the Born operator with the Hamiltonian of the atom, the first Born amplitude (2) can be written in the velocity gauge [23]. Close agreement between calculations performed with the two gauges of the Born operator, length and velocity, serves as a convenient test of the accuracy of the wave functions Ψ_0 and Ψ_f . The treatment of the first Born amplitude within the CCC formalism is given by Kheifets et al. [14].

Similarly to Eq. (2), we write the second Born amplitude as

$$\begin{aligned} f^{B2} &= \int d\mathbf{k} \sum_n \frac{\langle \mathbf{k}_1 \Psi_f(\mathbf{k}_2) | U | \mathbf{k} \Psi_n \rangle \langle \mathbf{k} \Psi_n | U | \mathbf{k}_0 \Psi_0 \rangle}{E_0 + k_0^2/2 - E_n - k^2/2 + i\delta} \\ &= \frac{1}{(2\pi)^6} \int d\mathbf{k} \frac{4\pi}{q_0^2} \frac{4\pi}{q_1^2} \sum_n \frac{\langle \Psi_f(\mathbf{k}_2) | e^{i\mathbf{q}_0 \mathbf{r}} + e^{i\mathbf{q}_0 \mathbf{r}'} - 2 | \Psi_n \rangle \langle \Psi_n | e^{i\mathbf{q}_1 \mathbf{r}} + e^{i\mathbf{q}_1 \mathbf{r}'} - 2 | \Psi_0 \rangle}{k_n^2/2 - k^2/2 + i\delta} \end{aligned} \quad (4)$$

Here $\mathbf{q}_0 = \mathbf{k}_0 - \mathbf{k}$ and $\mathbf{q}_1 = \mathbf{k} - \mathbf{k}_1$. The total momentum transfer $\mathbf{q}_0 + \mathbf{q}_1 = \mathbf{q}$. In the energy denominator we introduced $k_n^2/2 = E_0 + k_0^2/2 - E_n$. As compared to the first Born amplitude, Eq. (4) contains an additional integration over the momentum of the projectile in the intermediate state \mathbf{k} as well as the summation and integration over the intermediate states of the target n . Direct evaluation of Eq. (4) is not possible at present and further approximations ought to be made. We assume that all intermediate states of the target between two subsequent interactions with the projectile are equally probable and weight them with an average energy denominator (the so-called closure approximation). This allows us to use the closure relation and to perform a summation:

$$\sum_n \frac{|\Psi_n(\mathbf{r}, \mathbf{r}')\rangle \langle \Psi_n(\mathbf{x}, \mathbf{x}')|}{E_0 + k_0^2/2 - E_n - k^2/2 + i\delta} \approx \frac{\delta(\mathbf{r} - \mathbf{x}) \delta(\mathbf{r}' - \mathbf{x}')}{\bar{k}_n^2/2 - k^2/2 + i\delta}, \quad (5)$$

where $\bar{k}_n^2/2 = k_0^2/2 - \Delta E$ and $\Delta E = \bar{E}_n - E_0$ is an average excitation energy. This approximation was employed by many authors, most recently by Marchalant et al. [5] and Fang and Bartschat [6] in their calculations of the electron impact ionization-excitation of He. The validity of the closure approximation hinges on the assumption that the result is insensitive to the concrete choice of the average excitation energy ΔE . Earlier applications of the second Born model with the closure approximation were focused on the excitation-ionization processes. In these applications it was logical to set Δ close to the lowest most dominant excitation energy. In our case we intend to apply the second Born model to double ionization. In this case we found it more practical to set $\bar{k}_n = (k_0 k_1)^{1/2}$. We tested that for ionization-excitation processes this choice produced almost identical results to those gener-

ated by the fixed Δ recipe. Due to complicated structure of the second Born amplitude (4), it was evaluated only in the length gauge.

After having adopted the closure approximation, we still have to deal with the \mathbf{k} -integration in the second Born amplitude. In the majority of the reported second Born works, this integration was performed numerically by various brute force algorithms. Unfortunately, due to a very computationally intensive CCC part, we cannot implement any of those methods. Instead, we perform an analytical angular integration over all possible directions of the \mathbf{k} -vector. To achieve this, we follow Franz and Altick [24] and make use of the dipole approximation in the second Born amplitude. We make a partial wave expansion of the Born operator

$$e^{i\mathbf{q}\mathbf{r}} - 1 = 4\pi \sum_{LM} i^L [j_L(qr) - \delta_{L0}] Y_{LM}^*(\hat{r}) Y_{LM}(\hat{q}) \quad (6)$$

and restrict summation over the angular momentum to the $L = 1$ term. It was argued in Ref. [24] that this is justifiable as long as the momentum transfer from the projectile to the target q is small. In this case small q_0 and q_1 are likely to dominate the amplitude (4) because of the rapidly decreasing factors q_0^{-2} and q_1^{-2} . The spherical Bessel functions are known to be parametrically small $j_L(x) \propto x^L$, $j_0(x) - 1 \propto x^2$ [25]. Therefore, the dipole term is expected to be leading as long as the argument of the Bessel function is small. Franz and Altick [24] made the further approximation by taking the optical limit of the dipole term $j_1(x) \rightarrow x/3$. We will follow their derivation to demonstrate that this approximation is, in fact, wrong and leads to a significant overestimation of the second Born amplitude.

In the dipole approximation, taken to the optical limit, the second Born amplitude (4) becomes

$$f^{B2} \propto \int d\mathbf{k} \frac{\langle \Psi_f(\mathbf{k}_2) | (\mathbf{q}_0\mathbf{r} + \mathbf{q}_0\mathbf{r}') (\mathbf{q}_1\mathbf{r} + \mathbf{q}_1\mathbf{r}') | \Psi_0 \rangle}{|\mathbf{k}_0 - \mathbf{k}|^2 |\mathbf{k} - \mathbf{k}_1|^2 (k_n^2 - k^2 + i\delta)} \quad (7)$$

Having in mind the explicit symmetry of the two-electron wave function with respect to the interchange of \mathbf{r} and \mathbf{r}' , we can isolate two distinct terms in the the second Born amplitude:

$$\begin{aligned} f^{B2a} &\propto 2 \int d\mathbf{k} \frac{\langle \Psi_f(\mathbf{k}_2) | (\mathbf{q}_0\mathbf{r} \cdot \mathbf{q}_1\mathbf{r}') | \Psi_0 \rangle}{|\mathbf{k}_0 - \mathbf{k}|^2 |\mathbf{k} - \mathbf{k}_1|^2 (k_n^2 - k^2 + i\delta)} \\ f^{B2b} &\propto 2 \int d\mathbf{k} \frac{\langle \Psi_f(\mathbf{k}_2) | (\mathbf{q}_0\mathbf{r}' \cdot \mathbf{q}_1\mathbf{r}) | \Psi_0 \rangle}{|\mathbf{k}_0 - \mathbf{k}|^2 |\mathbf{k} - \mathbf{k}_1|^2 (k_n^2 - k^2 + i\delta)} \end{aligned}$$

We make use of the expansion

$$\mathbf{q}_0\mathbf{r} = q_0 r \cos(\hat{\mathbf{q}}_0 \hat{\mathbf{r}}) = \frac{4\pi}{3} q_0 r \sum_{m=-1}^1 Y_{1m}^*(\hat{\mathbf{r}}) Y_{1m}(\hat{\mathbf{q}}_0) \quad (8)$$

and, following Varshalovich [26], decouple vectors \mathbf{k} and \mathbf{k}_0 :

$$q_0 Y_{1m}(\hat{\mathbf{q}}_0) = \sqrt{4\pi} \sum_{\lambda=0}^1 \sum_{|\mu| \leq \lambda} (-1)^\lambda k^\lambda k_0^{1-\lambda} Y_{\lambda\mu}(\hat{\mathbf{k}}) Y_{1-\lambda m-\mu}(\hat{\mathbf{k}}_0) \quad (9)$$

For the same purpose, we make an expansion in the denominator:

$$\frac{1}{|\mathbf{k}_0 - \mathbf{k}|^2} = \frac{4\pi}{2k_0 k} \sum_{LM} Q_L \left(\frac{k_0^2 + k^2}{2kk_0} \right) Y_{LM}^*(\hat{\mathbf{k}}) Y_{LM}(\hat{\mathbf{k}}_0) \quad (10)$$

where Q_L is the Legendre polynomial of the second kind.

Combining expansions (8-10) allows us to perform an analytical integration over the direction of the \mathbf{k} -vector:

$$\int d\Omega_k \frac{(\mathbf{q}_0 \mathbf{r}) \cdot (\mathbf{q}_1 \mathbf{r}')}{|\mathbf{k}_0 - \mathbf{k}|^2 |\mathbf{k} - \mathbf{k}_1|^2} = \frac{(4\pi)^4}{36} r r' \sum_{mm'} Y_{1m}^*(\hat{\mathbf{r}}) Y_{1m'}^*(\hat{\mathbf{r}}') \mathcal{M}_{mm'}(k, k_0, k_1, \theta_1) \quad (11)$$

where

$$\begin{aligned} \mathcal{M}_{mm'}(k, k_0, k_1, \theta_1) &= \sum_{\lambda\mu} \sum_{\lambda'\mu'} (-1)^{\lambda+\lambda'} k^{\lambda+\lambda'-2} k_0^{-\lambda} k_1^{-\lambda'} \\ &\quad Y_{1-\lambda m-\mu}(\hat{\mathbf{k}}_0) Y_{1-\lambda' m'-\mu'}(\hat{\mathbf{k}}_1) \sum_{JM_J} \hat{\lambda} \hat{\lambda}' \hat{J}^{-2} C_{\lambda 0, \lambda' 0}^{J 0} C_{\lambda\mu, \lambda'\mu'}^{JM_J} \\ &\quad \sum_{LM} \sum_{L'M'} Q_L \left(\frac{k_0^2 + k^2}{2kk_0} \right) Q_{L'} \left(\frac{k_1^2 + k^2}{2kk_1} \right) \hat{L} \hat{L}' C_{LM, L'M'}^{JM_J} C_{L 0, L' 0}^{J 0} Y_{LM}(\hat{\mathbf{k}}_0) Y_{L'M'}(\hat{\mathbf{k}}_1) \end{aligned} \quad (12)$$

Here we used the standard notation for the Clebsch-Gordan coefficients and introduced the hat-function $\hat{J} = (2J + 1)^{1/2}$. In writing the argument of the function $\mathcal{M}_{mm'}(k, k_0, k_1, \theta_1)$ we assumed that the z -axis is aligned along the direction of the incident projectile $\hat{\mathbf{k}}_0$ which scatters at the angle θ_1 in the xz plane. Summation over L, L' should be terminated at some large value L_{cut} when desired numerical accuracy is achieved. In practical computations, we used the cut-off values of the order of few hundred, the higher incident energy requiring the larger L_{cut} .

After performing the angular integration we can present the two parts of the second Born amplitude as

$$\begin{aligned} f^{B2a} &\propto \frac{(4\pi)^4}{18} \sum_{mm'} \langle \Psi_f(\mathbf{k}_2) | r r' Y_{1m}^*(\hat{\mathbf{r}}) Y_{1m'}^*(\hat{\mathbf{r}}') | \Psi_0 \rangle \int k^2 dk \frac{\mathcal{M}_{mm'}(k, k_0, k_1, \theta_1)}{k_n^2 - k^2 + i\delta} \\ &= \frac{(4\pi)^4}{18} \sum_{mm'} \overline{\mathcal{M}}_{mm'}(k_0, k_1, \theta_1) \langle \Psi_f(\mathbf{k}_2) | r r' Y_{1m}^*(\hat{\mathbf{r}}) Y_{1m'}^*(\hat{\mathbf{r}}') | \Psi_0 \rangle \end{aligned} \quad (13)$$

Here we introduced an integrated kinematical factor (IKF):

$$\overline{\mathcal{M}}_{mm'}(k_0, k_1, \theta_1) = \int k^2 dk \frac{\mathcal{M}_{mm'}(k, k_0, k_1, \theta_1)}{k_n^2 - k^2 + i\delta}$$

Similarly,

$$f^{B2b} \propto \frac{(4\pi)^4}{18} \sum_{mm'} \overline{\mathcal{M}}_{mm'}(k_0, k_1, \theta_1) \langle \Psi_f(\mathbf{k}_2) | r^2 Y_{1m}^*(\hat{\mathbf{r}}) Y_{1m'}^*(\hat{\mathbf{r}}) | \Psi_0 \rangle \quad (14)$$

Great advantage of Eqs. (13-14) is that the IKF is separated from the matrix elements which contain the spatial integration of the initial and final state wave functions. Therefore the IKF can be calculated once and for all the second Born matrix elements.

Spatial integrals can be evaluated by the configuration-interaction expansion of the ground state

$$\Psi_0(\mathbf{r}, \mathbf{r}') = \sum_{n_i l_i m_i} C_{n_i l_i} \frac{1}{\hat{l}_i} (-1)^{l_i - m_i} Y_{l_i m_i}(\hat{\mathbf{r}}) \frac{1}{r} P_{n_i l_i}(r) Y_{l_i - m_i}(\hat{\mathbf{r}}') \frac{1}{r'} P_{n_i l_i}(r'), \quad (15)$$

and the close-coupling expansion of the final state

$$\Psi_f(\mathbf{k}_2) = \psi_f(\mathbf{k}_2) + \sum_n \sum_{\mathbf{k}} \frac{\langle \mathbf{k}_2 f | T | n \mathbf{k} \rangle \psi_n(\mathbf{k})}{k_f^2/2 + \epsilon_f - k^2/2 - \epsilon_n + i\delta} \quad (16)$$

with the channel function further expanded over the partial waves:

$$\psi_f(\mathbf{k}, \mathbf{r}, \mathbf{r}') = \frac{1}{k^{1/2}} \sum_{lm} e^{-i\delta_l} i^l Y_{lm}^*(\hat{\mathbf{k}}) Y_{lm}(\hat{\mathbf{r}}) \frac{1}{r} P_{El}(r) Y_{l_f m_f}(\hat{\mathbf{r}}') \frac{1}{r'} P_{n_f l_f}(r'). \quad (17)$$

In Eq. (15), $C_{n_i l_i}$ are the configuration interaction coefficients and $\hat{l}_i^{-1} (-1)^{l_i - m_i} \equiv C_{l_i m_i l_i - m_i}^{00}$.

In Eq. (16), $\langle \mathbf{k}_2 f | T | n \mathbf{k} \rangle$ is the half-on-shell T -matrix (see Ref. [14] for more details).

After performing the spherical integration and applying some angular momentum algebra we can write the second Born amplitude in the form:

$$\begin{aligned} \langle \psi_f(\mathbf{k}) | f^{B2} | \Psi_0 \rangle &= \frac{1}{k^{1/2}} \frac{3}{4\pi} \sum_{lm} e^{i\delta_l} i^{-l} Y_{lm}(\hat{\mathbf{k}}) \\ &\sum_{JM_J} \hat{J} \begin{pmatrix} l & J & l_f \\ m & M_J & m_f \end{pmatrix} \mathcal{M}_{JM_J}(k_0, k_1, \theta_1) \left[D_{lJf}^{(2a)}(k) + D_{lJf}^{(2b)}(k) \right] \end{aligned} \quad (18)$$

Here we introduced the reduced matrix elements

$$D_{lJf}^{(2a)}(k) = \sum_{n_i l_i} C_{n_i l_i} \hat{l}_i \hat{l}_f \begin{pmatrix} l & 1 & l_i \\ 0 & 0 & 0 \end{pmatrix} \begin{pmatrix} l_f & 1 & l_i \\ 0 & 0 & 0 \end{pmatrix} (-1)^J \begin{Bmatrix} 1 & J & 1 \\ l & l_i & l_f \end{Bmatrix} \int dr P_{kl}(r) r P_{n_i l_i}(r) \int dr' P_{n_f l_f}(r') r' P_{n_i l_i}(r') \quad (19)$$

$$D_{lJf}^{(2b)}(k) = \sum_{n_i l_i} C_{n_i l_i} (-1)^{l_i} \hat{l} \begin{pmatrix} l & J & l_i \\ 0 & 0 & 0 \end{pmatrix} \begin{pmatrix} 1 & 1 & J \\ 0 & 0 & 0 \end{pmatrix} \int dr P_{kl}(r) r^2 P_{n_i l_i}(r) \int dr' P_{n_f l_f}(r') P_{n_i l_i}(r') \quad (20)$$

and coupled the IKF to the total angular momentum and its projection:

$$\sum_{m,m'} C_{1m,1m'}^{JM} \overline{\mathcal{M}}_{mm'}(k_0, k_1, \theta_1) \equiv \mathcal{M}_{JM}(k_0, k_1, \theta_1)$$

The second Born amplitude (7) is to be added to the first Born amplitude:

$$\langle \psi_f(\mathbf{k}) | f^{B1} | \Psi_0 \rangle = \frac{\sqrt{4\pi}}{k^{1/2}} \sum_{Jlm} e^{i\delta_l} j^{J-l} Y_{lm}(\hat{k}) Y_{JM_J}(\hat{q}) \begin{pmatrix} l_f & J & l \\ m_f & M_J & m \end{pmatrix} \hat{J} D_{lJf}(q, E) \quad (21)$$

where a reduced first Born matrix element

$$D_{lJf}^{(1)}(q, E) = \sum_{n_i l_i} C_{n_i l_i} (-1)^{l_i} \hat{l} \begin{pmatrix} l & J & l_i \\ 0 & 0 & 0 \end{pmatrix} \int dr P_{El}(r) j_J(qr) P_{n_i l_i}(r) \int dr' P_{n_f l_f}(r') P_{n_i l_i}(r') \quad (22)$$

Unlike the dipole-only second Born term, we include all numerically significant multipoles to the first Born amplitude. Exchange terms obtained by swapping the continuum state \mathbf{k} and the discrete state f are included in Eqs. (19), (20) and (22) but not shown for brevity. The matrix elements (7) and (21) are calculated with the channel function $\psi_f(\mathbf{k})$. When the close-coupling final state $\Psi_f(\mathbf{k}_2)$ is constructed from the channel functions, as prescribed by Eq. (16), these matrix elements should be integrated with the half-on-shell T -matrix [14].

B. Validity of the optical limit

As we already mentioned, Franz and Altick [24] took the dipole approximation for the second Born amplitude to its dipole limit. Here we demonstrate that this approximation is too crude and needs to be corrected. We make a partial wave expansion of the \mathbf{q} -dependent part of the second Born operator:

$$\begin{aligned} \hat{f}^{B2a} &\propto \int d\Omega_k \exp(i\mathbf{q}_0 \mathbf{r}) \exp(i\mathbf{q}_1 \mathbf{r}') q_0^{-2} q_1^{-2} \\ &\propto (4\pi)^2 \sum_{l'l'} i^{l+l'} \int d\Omega_k j_l(q_0 r) j_{l'}(q_1 r') \mathcal{Y}_{l'l'}^{JM}(\mathbf{q}_0, \mathbf{q}_1) q_0^{-2} q_1^{-2} \end{aligned} \quad (23)$$

Here we introduced a bipolar spherical harmonics [26]

$$\mathcal{Y}_{l'l'}^{JM}(\mathbf{q}_0, \mathbf{q}_1) = \sum_{mm'} C_{lm,l'm'}^{JM} Y_{lm}(\mathbf{q}_0) Y_{l'm'}(\mathbf{q}_1)$$

Another second Born operator \hat{f}^{B2b} will have a similar expansion in which $r = r'$.

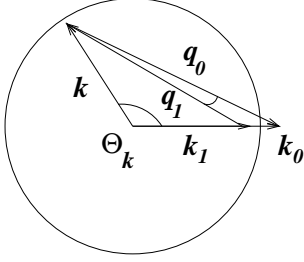


FIG. 1: Vectors of the momentum transfer in the second Born process.

As we restrict ourselves to the dipole terms $l = l' = 1$, the total momentum $J = 0$ or 2 . In the optical limit, $j_1(qr) = qr/3$ and we are able to separate the spatial \mathbf{r}, \mathbf{r}' integration and the angular $\hat{\mathbf{k}}$ integration in the second Born term. To justify this approximation we rely on a very rapid fall of the $q_0^{-2}q_1^{-2}$ factor. A typical configuration of the vectors $\mathbf{k}_0, \mathbf{k}_1$ and \mathbf{k} is exhibited in Fig. 1. As the scattering angle of the fast projectile is usually small, the vectors \mathbf{k}_0 and \mathbf{k} are almost collinear. For most orientations of the vector \mathbf{k} both vectors \mathbf{q}_0 and \mathbf{q}_1 are large, of the order of \mathbf{k}, \mathbf{k}_0 , and the cut-off factor $q_0^{-2}q_1^{-2}$ is small indeed. However, in a narrow angular range near $\theta_{\mathbf{k}} = 0$, both \mathbf{q}_0 and \mathbf{q}_1 small and the cut-off factor is inefficient. Here the validity of the optical limit will depend on how far the radial integration over r, r' should be extended.

To investigate this matter in more detail we explore the ratio of the two radial functions $z(r) = P(r)/R(r)$ where

$$P(r) = \int_{-1}^1 d \cos \theta_{\mathbf{k}} j_1(q_0 r) j_1(q_1 r) \mathcal{Y}_{11}^{J0}(\mathbf{q}_0, \mathbf{q}_1) q_0^{-2} q_1^{-2} \quad (24)$$

$$R(r) = \frac{r^2}{9} \int_{-1}^1 d \cos \theta_{\mathbf{k}} \mathcal{Y}_{11}^{J0}(\mathbf{q}_0, \mathbf{q}_1) q_0^{-1} q_1^{-1} .$$

These functions contain the azimuthal angle integrals of the full dipole term and with its optical limit, respectively. We choose $M_J = 0$ as this term will be leading due to an approximate axial symmetry. The ratio $z(r)$ is shown in Fig. 2 for $J = 0$ and $J = 2$. We

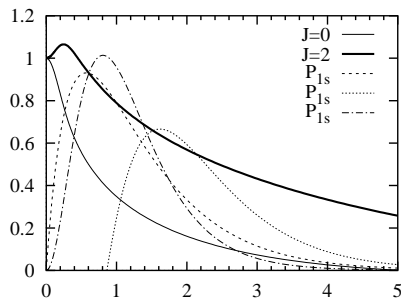


FIG. 2: Deviation from the optical limit measured as ratio $z(r) = P(r)/R(r)$ shown as thin and thick solid lines for $J = 0$ and 2 , respectively. The kinematics of Avaldi et al. [21] is chosen with an impact energy of 570 eV. The He atom orbitals P_{1s}, P_{2s} (positive half-wave) and P_{2p} from the MCHF ground state are shown on the same radial scale.

see that the ratio is indeed close to unity for very small $r < 1$ a.u. but then it rapidly falls off, the $J = 0$ term being effected particularly strongly. In the same figure we show, for illustration, the radial orbitals from the helium atom ground state calculated in the multi-configuration Hartree-Fock (MCHF) approximation. We see that the radial extent of these orbitals, especially P_{2p} , is such that the radial factor is significantly below unity which indicates significant overestimation of the second Born term taken to the optical limit, particularly in the monopole channel.

To counter this deficiency of the present formalism but to retain a convenience of the separate \mathbf{q} and r integrations, we propose the following computational scheme. We add the factor $z(r)$ to the radial integral $\int dr P_{kl}(r) r^2 P_{n_i l_i}(r)$ in the reduced matrix element (20). Similarly, we introduce a factor $z(r, r')$, calculated with the same expressions (24) but $r \neq r'$, into the reduced matrix element (19). As all the radial orbitals entering Eqs. (19-20) are defined on a standard radial grid r_i , we have to calculate a vector z_i and a matrix z_{ij} only once and then use them in all subsequent radial integrations.

III. RESULTS AND DISCUSSION

A. Ionization with excitation

Electron-impact ionization-excitation of He leading to the $n = 2$ excited state is a very convenient test case. For this process, a large volume of experimental and theoretical data exists which can be used to calibrate our model. Dupré et al. [20] reported their ionization-excitation measurement at $E_0 \simeq 5.5$ keV and $E_2 = 5, 10$ and 75 eV. The first Born results for the two lowest electron energies of 5 and 10 eV are well below the experiment and only for the 75 eV case is agreement with experiment satisfactory [3, 4]. The second Born calculations [5, 6] are somewhat closer to experiment but significant discrepancies still exist for the two lowest ejected electron energies. Nevertheless, these calculations provide us with a useful benchmark to test our model.

In Fig. 3 we show our first and second Born results for the experiment of Dupré et al. [20] along with the R -matrix calculations with pseudostates (RMPS) by Fang and Bartschat [6]. Except for the lowest ejected electron energy of 5 eV, both our first and second Born results are very close to those produced by the RMPS model. This agreement is satisfying

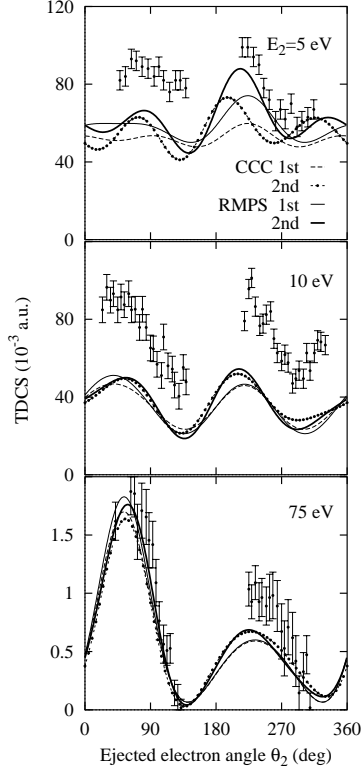


FIG. 3: Fully resolved triply differential cross-section (TDCS) of the ionization-excitation of He leading to the $n = 2$ excited state. Kinematics corresponds to the experimental setup of Dupré et al. [20]. CCC calculations in the first and second Born models are shown by the dashed and dotted lines, respectively. Analogous calculations in the RMPS model [6] are shown accordingly by the thin and thick solid lines. The energy of the ejected electron $E_2 = 5, 10$ and 75 eV from top to bottom panels.

since the CCC and RMPS models rely on different set of approximations. The RMPS model does not restrict the second Born term to the dipole contribution. Instead, it reduces the integration over the energy of the projectile in the intermediate state to a single on-shell point, i.e. only the imaginary part of the integral (7) is taken. In our model, both the real and imaginary parts of the integrals (7) and (13) are included. Although, the imaginary part is indeed systematically larger than its real counterpart.

In the case of the lowest 5 eV energy, the first Born calculations in the CCC and RMPS models disagree. This is most likely due to a very strong sensitivity of the cross-section to the ejected electron energy which falls into the region of the autoionizing resonances [27]. It is therefore not surprising that our second Born results deviate from those of the RMPS method. Nevertheless, the direction and the amount of change caused by the second Born correction is similar in both calculations. We should stress that the second Born corrections are generally small at such a large impact energy as 5.5 keV. We will make a similar observation for the double ionization process at the same impact energy.

The ionization-excitation experiments of Avaldi et al. [21] were performed at a much lower incident energy (0.6–1.5 keV) than those of Dupré et al. [20]. Consequently, much stronger second Born effects were theoretically predicted for this kinematics [5, 6]. Therefore, this

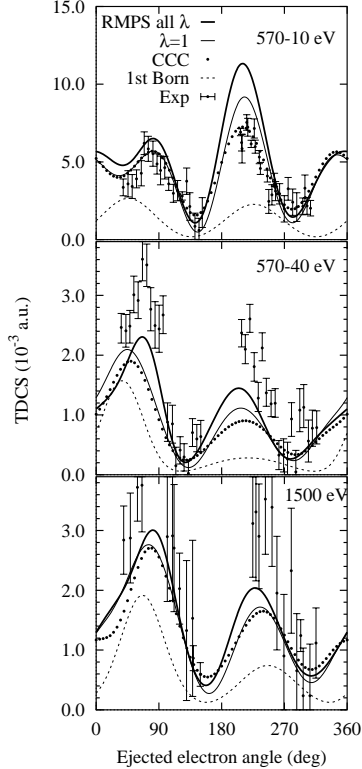


FIG. 4: TDCS of the ionization-excitation of He corresponding to the experimental setup of Avaldi et al. [21]. The energy of the scattered/ejected electron pair E_1/E_2 is 570/10, 570/40 and 1500/20 eV from top to bottom panels. The RMPS calculations [6] with full and dipole only second Born term are shown by thick and thin solid lines, respectively.

kinematics provides us with a more challenging test to assure the accuracy of our model. In Fig. 4 we show our first and second Born calculations for various kinematics of the experiment of Avaldi et al. [21] in comparison with RMPS calculation of Fang and Bartschat [6]. The CCC first Born results are almost identical to those of RMPS and both calculations are shown as a single dashed line. The second Born results in the RMPS model are shown with all the multipoles included (thick solid line) as well as the dipole-only second Born term (thin solid line). The CCC model is only available with the dipole-only second Born contribution and it is shown by the dotted line. We see that both dipole models produce very close results. Therefore the difference between CCC and RMPS is primarily due to limitation of the former to the dipole contribution to the second Born term. The difference between the first and second Born results is much larger than the difference between the dipole-only and all-multipoles-included second Born calculations. This indicates that the dipole contribution is indeed leading in the second Born term.

B. Double ionization by electron impact

Having tested the accuracy of our approach we are in a position to apply the second Born CCC model to double ionization processes. We start with double ionization of He by electron impact which can now be studied experimentally with fully resolved kinematics of all three electrons involved in the collision, the process known as the (e,3e) reaction. We begin comparison with experiment by selecting the highest incident energy of 5.5 keV reported in a series of publications by Lahmam-Bennani and co-workers [8, 14, 28]. In these experiments, all three electrons were bound to the scattering plane and the fully-resolved five-fold differential cross-section (FDCS) was measured as a function of the azimuthal angles of the two ejected electrons θ_2, θ_3 .

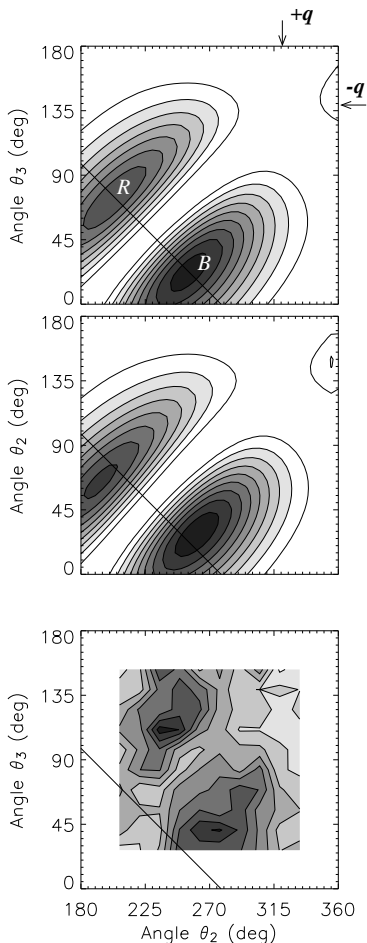


FIG. 5: FDCS of (e,3e) on He at $E_0 = 5.5$ keV and $E_2 = E_3 = 10$ eV. The top panel - first Born calculation, middle panel - second Born calculation, bottom panel - experiment of Taouil et al. [28]. The cross-sections are exhibited as filled contour plots with the escape angles θ_2 and θ_3 shown on the axes. The areas of large cross-section are indicated by darker shades of grey. The first Born FDCS has a \mathbf{q} symmetry axis indicated as a straight line. Only the experimentally accessible angular range is shown.

In Fig. 5 and 6 we present our first and second Born calculations for the ejected electron energies of $E_2 = E_3 = 10$ eV and $E_2 = E_3 = 4$ eV, respectively. We display the data as density plots with the angles θ_2, θ_3 shown on the axes and the FDCS indicated by various

shades of gray, the darker shade representing a larger cross-section. As the double ionization events are fairly rare, statistics of the (e,3e) experiments is usually limited and the error bars are quite large. In this situation, the 2D density plots give a clearer view of the data as compared to one-dimensional cuts through the fixed angles θ_2 or θ_3 as was used by Lahmam-Bennani and co-workers. The sign convention of the present experiment is that the scattering angle of the projectile is positive $\theta_1 > 0$ and the momentum transfer angle is negative $\theta_q < 0$. This choice, however, is not universal and other (e,3e) experiments considered in this paper have opposite sign convention $\theta_q > 0$. To avoid confusion, we always mark the direction of the momentum transfer \mathbf{q} when showing our results.

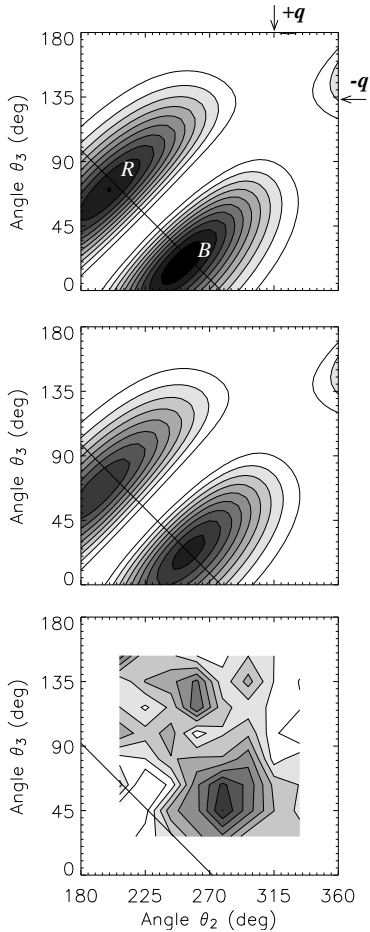


FIG. 6: Same as in Fig. 5 for $E_0 = 5.5$ keV and $E_2 = E_3 = 4$ eV. Experiment is reported in Ref. [14].

Because of a large incident energy and a low momentum transfer, the experiments of Lahmam-Bennani and co-workers can be conveniently analyzed in comparison with a simpler process of double ionization by photon impact known as the $(\gamma,2e)$ reaction [8]. This analysis is particularly transparent when the data are viewed as 2D density plots [7, 15]. The two-peak cross-section pattern displayed in Figs. 5 and 6 is formed by the dipole selection rules

(rigid in $(\gamma, 2e)$ but somewhat relaxed in low- q ($e, 3e$)) and the exchange symmetry of equal energy electrons which excludes the parallel emission $\theta_2 = \theta_3$. In the case of $(\gamma, 2e)$, when the momentum transfer is vanishing, the two peaks are identical. At finite \mathbf{q} , these two peaks can be distinguished as binary (marked B) and recoil (marked R). In the binary peak, the sum of the ejected electron momenta $\mathbf{K} = \mathbf{k}_2 + \mathbf{k}_3$ is aligned with the $+\mathbf{q}$ direction whereas in the recoil peak the \mathbf{K} vector is pointed approximately to the $-\mathbf{q}$ direction. In the first Born model, the momentum transfer vector \mathbf{q} provides a natural symmetry axis to the cross-section which is indicated as a straight line in Figs. 5 and 6. On this line, the two electrons are ejected symmetrically on the opposite side with respect to the momentum transfer direction $\theta_2 - \theta_{\mathbf{q}} = -(\theta_3 - \theta_{\mathbf{q}})$. In the CCC implementation of the first Born model, the binary peak is somewhat larger than the recoil one. It is just the reverse in the first Born model based on the asymptotically exact Coulomb wave functions (BBK) [7].

As is seen on the middle panel of Figs. 5 and 6, the second Born corrections remove the symmetry with respect to the momentum transfer direction pushing the binary and recoil peaks to the opposite side of the $\hat{\mathbf{q}}$ axis. Apart from this small shift, no appreciable change can be seen in the FDCS. Unfortunately, the experimental data have limited statistics as well as restricted angular range to support or reject these theoretical findings unambiguously. At 10 eV ejected electrons energy, the binary peak seems to be at the right position but the recoil peak is significantly misplaced. This displacement, however, cannot be stated categorically since the theoretically predicted angular position of the recoil peak is not accessible experimentally. At 4 eV ejected electrons energy, the binary peak in the experiment is shifted much stronger from the $\hat{\mathbf{q}}$ axis as compared to the theory. The recoil peak is either missing due to a narrow accessible angular range, or too weak and misplaced, as compared with the calculation.

A more definitive comparison with experiment can be performed at a lower incident energy of 2 keV where the second Born effects become stronger. The $(e, 3e)$ measurements at this energy were reported by Dorn et al. [15, 16]. This group employed the COLTRIMS method which allowed, in principle, to sample the full angular range of the two ejected electrons. The only limitation was imposed by the time-of-flight technique which excluded detection of the two ejected electrons arriving at the detector at close times (the so-called detector dead time). This arrival, however, was not very likely and only the area of a relatively small cross-section was omitted from experiment.

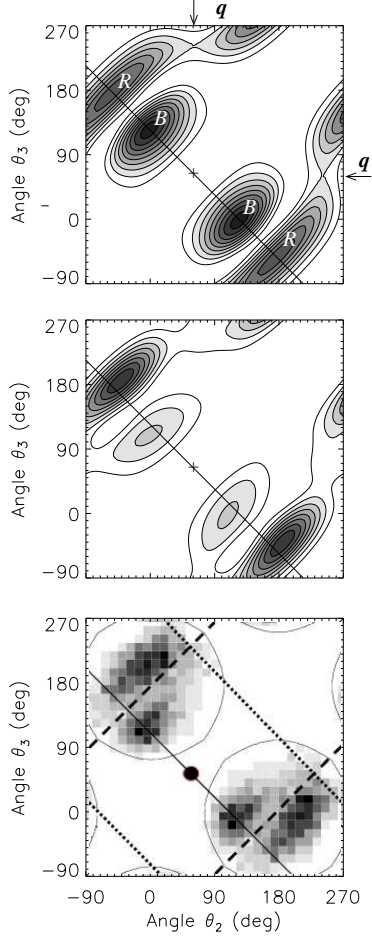


FIG. 7: FDCS of (e,3e) on He at $E_0 = 2$ keV and $E_2 = E_3 = 5$ eV. Experiment is reported in Ref. [15]. Straight dotted lines in the experimental plot indicate the nodal lines due to the dipole selection rules. The angular range which is not affected by the detector dead-time is encircled by solid lines. The width of a filled circle on the \mathbf{q} - symmetry line indicates experimental uncertainty of the direction of the momentum transfer.

In Fig. 7 we show the first and second Born calculations for $E_0 = 2$ keV and $E_2 = E_3 = 5$ eV in comparison with the experimental data of Dorn et al. [15]. Here the full angular range of θ_2, θ_3 allows to display two pairs of the binary (B) and recoil (R) peaks which are symmetric due to indistinguishability of the two ejected electrons. In the first Born model (top panel), all the peaks are symmetric relative to the momentum transfer axis, shown as a solid line. More intensity goes into the binary peak whereas the recoil peak is weaker and has a slightly elongated shape. When the second Born corrections are included (middle panel), the binary peak loses much of its intensity which is transferred to the recoil peak. Both peaks, especially the recoil one, are displaced relative to the momentum transfer axis. Displacement of the recoil peak is clearly seen in the experiment (bottom panel). The binary peak remains approximately on the momentum transfer line. Its possible displacement could be masked by the experimental uncertainty in the momentum transfer direction (indicated by the width of the filled circle on the bottom panel). The experiment generally supports predictions of the second Born model except for the relative intensity of the B and R peaks

which have about the same strength.

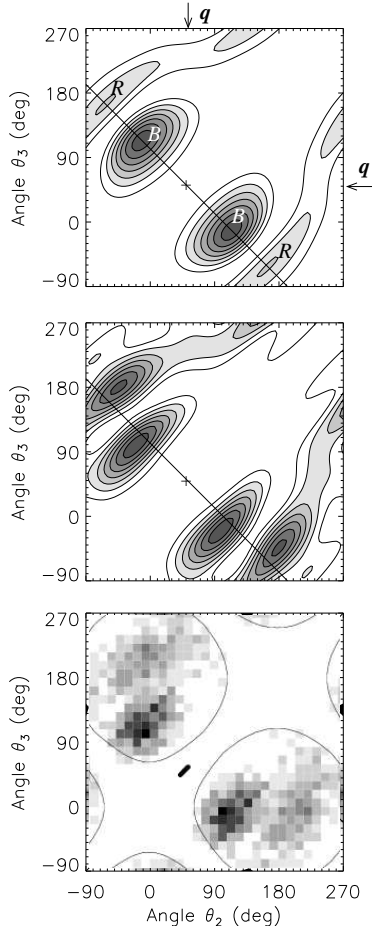


FIG. 8: Same as in Fig. 5 for $E_0 = 2$ keV and $E_2 = E_3 = 5$ eV. Experiment is reported in Ref. [15].

When the ejected electron energy is increased to $E_2 = E_3 = 20$ eV, the first Born calculation predicts nearly all the intensity going to the binary peak (see top panel of Fig. 8). This is so because the binary peak is enhanced by its proximity to the Bethe ridge where $\mathbf{k}_2 + \mathbf{k}_3 \simeq \mathbf{q}$. As in the previous case of $E_2 = E_3 = 5$ eV, inclusion of the second Born corrections transfers intensity from the binary peak to the recoil peak and shifts both peaks relative to the momentum transfer axis (middle panel of Fig. 8). This shift is seen in the experiment (bottom panel of Fig. 8), but the binary peak remains much more intense than the recoil one.

Finally, we consider the case of a very low incident energy of $E_0 = 0.5$ keV [18]. As can be expected from the previous analysis of ionization-excitation processes, at such a low incident energy the second Born effects become very strong. And indeed, as is seen from Fig. 9, the second Born corrections completely transform the FDCS pattern. The binary peak is all but disappear and both peaks are shifted strongly from the q symmetry line. The

experimental cross-section displays a very similar pattern.

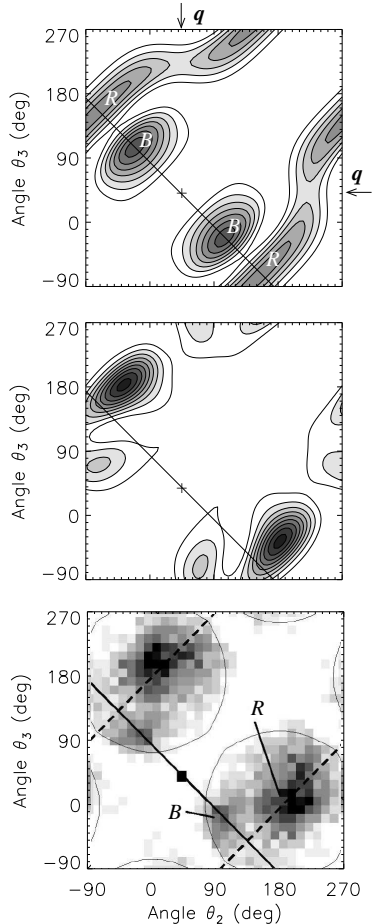


FIG. 9: Same as in Fig. 5 for $E_0 = 0.5$ keV and $E_2 = E_3 = 5$ eV. Experiment is reported in Ref. [18].

C. Double ionization by proton impact

The most prominent effect of the second Born corrections is the charge dependence of the particle impact ionization. The first Born amplitude is proportional to the projectile charge Z , the second Born amplitude is proportional to Z^2 and their cross-product term in the cross-section is proportional to Z^3 , i.e. it changes its sign when the charge of the projectile is reverted. That is why one expects to observe the difference between the particle and antiparticle induced ionization cross-sections. The counterpart of the (e,3e) would be positron induced double ionization. This reaction cannot be realized at present. However, the proton impact double ionization is now feasible with fully resolved kinematics.

Fischer et al. [19] reported FDCS of the proton impact ionization of He at the projectile velocity $V_0 = 15.5$ a.u. A similar velocity $V_0 = 12.2$ a.u. was used in the (e,3e) experiments

on He by Dorn et al. [15] and this allowed a straightforward comparison. The count rate was much lower in the proton induced double ionization and, to accumulate statistically significant data, Fischer et al. [19] had to accept all equal energy electron pairs with $E_2 = E_3 < 25$ eV binned into large intervals of the momentum transfer $q_{\min} < q < q_{\max}$. To make a comparison with electron impact double ionization, they also binned the (e,3e) data in a similar manner. When compared with each other, the proton data showed clear difference from their electron counterparts. The proton FDCS exhibited more first Born-like behavior with a very prominent binary peak nearly symmetric with respect to the direction of the momentum transfer.

To simulate the proton impact FDCS, we simply change the sign with which the first and second Born amplitudes interfere. That would amount to the positron impact double ionization in which the positronium formation and annihilation is neglected. In Fig. 10 we show our first and second Born calculations for the positron impact FDCS in comparison with the experimental data of Fischer et al. [19] taken at the lowest momentum transfer slice from 0.2 to 0.8 a.u. We cannot simulate larger momentum transfers since our dipole approximation relies on a small q . We represent the experimental interval of the momentum transfer by a single point $q = 0.6$ a.u. To investigate an ejected electrons energy dependence we performed two calculations at $E_2 = E_3 = 5$ and 20 eV. Unlike in the case of electron impact double ionization, we did not find significant difference between the second Born results at these two energies. In Fig. 10 we present the $E_2 = E_3 = 20$ eV calculation only.

The influence of the second Born effects is relatively weaker in the case of proton impact ionization as compared to (e,3e) under similar kinematical conditions (see Fig. 8). The Binary peak remains the dominant feature. The recoil peak is displaced from the q -symmetry line to the direction opposite as compared to the electron impact case. However, unlike in (e,3e), the recoil peak remains a weak feature relative to a very prominent binary peak. This predictions of theory are generally supported by experiment.

The authors of Ref. [19] interpreted this apparent closeness of the proton impact double ionization to the first Born regime by classical arguments. They speculated that the positively charged projectile would pull the target electron away from its parent nucleus shaking the second electron into the continuum, thereby increasing the probability of a clear binary peak. Our quantum mechanical calculations do not support this scenario. Except for their relative sign, the first and second Born amplitudes are exactly the same for the electron and

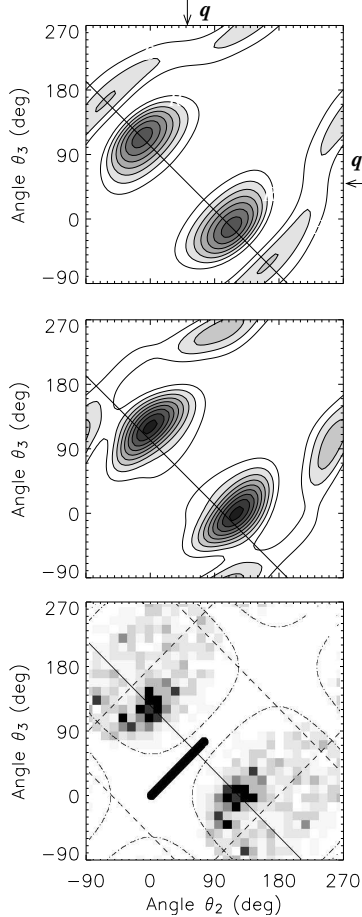


FIG. 10: FDCS of positron impact ionization of He at $E_0 = 2$ keV ($V_0 = 12.2$ a.u.), $q = 0.6$ a.u. and $E_2 = E_3 = 20$ eV. Top panel - first Born calculation, middle panel - second Born calculation, bottom panel - experiment on proton impact ionization with $V_0 = 15.5$ a.u., $0.2 < q < 0.8$ and $E_2 = E_3 < 25$ eV[19]. The solid line indicates the symmetry around the momentum transfer direction. This direction varies in the experiment and an average position is shown. The thick solid bar indicates possible deviation from this average position. The angular range which is not affected by the detector dead-time is encircled by dashed lines. The dipole nodal lines are shown as in Fig. 7.

proton impact, even though, the electron is pushing and the proton is pulling the target electron from its parent ion. Taken in separation, both amplitudes generate exactly the same double ionization cross-section with a positively and negatively charged projectiles. It is the interference of the first and second Born amplitudes which creates the difference between the electron and proton impact. This is a purely quantum effect and it cannot be interpreted classically.

IV. CONCLUSIONS AND FURTHER DIRECTIONS

In this paper we describe a theoretical model of charged particle impact ionization-excitation and double ionization based on the CCC representation of the final state with two active electrons. The novelty of this model is inclusion of the second Born processes in which the projectile interacts with the target repeatedly, ejecting two target electrons in sequence. We employ a number of approximations to treat the second Born amplitude, most notably, the dipole approximation which restricts the orbital momentum exchange be-

tween the projectile and the target to two dipole interactions. This approximation allows us to perform an analytical angular integration over the momentum of the projectile between these two interactions. The use of the analytical, rather than numerical, integration speeds up the computations considerably.

To assure the accuracy of the model, we make a comparison with well established theoretical and experimental data on the electron impact ionization-excitation of He leading to the $n = 2$ final state. As a benchmark, we use the RMPS theoretical results, both with the full and the dipole-only second Born term. The difference between these two calculations is not exceeding 30% and this gives us an indication of a typical accuracy of our model.

Having tested our model, we apply it to the electron and proton impact double ionization of He in kinematics of recent experiments. The (e,3e) experiments are chosen with the projectile energy ranging from 5.5 keV down to 0.5 keV. The first and second Born calculations indicate that the second Born effects vary from very weak to very strong across this incident energy range. The statistical quality of the experimental data at the highest incident energy does not allow to test predictions of the model unambiguously. The COLTRIMS data at the projectile energy of 2 keV, and especially at 0.5 keV, support our theoretical findings. The model also predicts accurately a strong deviation between the proton and electron impact double ionization at the same projectile velocity. This difference is attributed to the quantum interference of the first and second born amplitudes. We find this explanation more satisfactory rather than classical interpretation based on the direction of the force exerted by the projectile on the target electron.

Although we applied the model to He, the simplest two-electron target, the model can easily accommodate more complex atoms such as Be and Mg by employing the frozen-core approximation [29]. Other atomic targets such as outer valence shells of noble gas atoms can be treated in a similar way [30]. To improve the accuracy of the model, it would be beneficial to go beyond the dipole approximation and to treat the second Born amplitude in full. This would also allow to describe the large \mathbf{q} processes. The work in this direction is currently underway.

In a broader context, it would be desirable to abandon the Born approximation altogether and to treat the four-body Coulomb final state non-perturbatively. Within the CCC formalism, this would require construction of a channel function build as a product of a Coulomb wave and two pseudostates. Some preliminary results in this directions have been

reported by Plottke et al. [31].

Acknowledgments

During the work on this project, the author received invaluable advise and help from many colleagues and friends, experimentalists and theorists alike. In particular, the author wishes to mention Igor Bray, Klaus Bartschat, Alexander Dorn, Azzedin Lahmam-Bennani and Daniel Fischer.

The Australian Partnership for Advanced Computing is acknowledged for providing access to the Compaq AlphaServer SC National Facility.

-
- [1] J. Berakdar, A. Lahmam-Bennani, and C. D. Cappello, *Phys. Rep.* **374**(2), 91 (2003).
- [2] H. R. J. Walters, *Phys. Rep.* **116**(1-2), 1 (1984).
- [3] A. Kheifets, I. Bray, and K. Bartschat, *J. Phys. B* **32**(15), L433 (1999).
- [4] P. J. Marchalant, J. Rasch, C. T. Whelan, D. H. Madison, and H. R. J. Walters, *J. Phys. B* **32**(24), L705 (1999).
- [5] P. J. Marchalant, C. T. Whelan, and H. R. J. Walters, *J. Phys. B* **31**(6), 1141 (1998).
- [6] Y. Fang and K. Bartschat, *J. Phys. B* **34**(2), L19 (2001).
- [7] A. S. Kheifets, I. Bray, J. Berakdar, and C. D. Cappello, *J. Phys. B* **35**(1), L15 (2002).
- [8] A. Lahmam-Bennani, I. Taouil, A. Duguet, M. Lecas, L. Avaldi, and J. Berakdar, *Phys. Rev. A* **59**(5), 3548 (1999).
- [9] S. Jones and D. H. Madison, *Phys. Rev. Lett.* **91** (2003).
- [10] R. Choubisa, G. Purohit, and K. K. Sud, *J. Phys. B* **36**(9), 1731 (2003).
- [11] R. E. Mkhater and C. D. Cappello, *J. Phys. B* **31**(2), 301 (1998).
- [12] J. R. Götz, M. Walter, and J. S. Briggs, *J. Phys. B* **36**(4), L77 (2003).
- [13] J. Berakdar, *Phys. Rev. Lett.* **85**(19), 4036 (2000).
- [14] A. S. Kheifets, I. Bray, A. Duguet, A. Lahmam-Bennani, and I. Taouil, *J. Phys. B* **32**(21), 5047 (1999).
- [15] A. Dorn, A. Kheifets, C. D. Schröter, B. Najjari, C. Höhr, R. Moshhammer, and J. Ullrich, *Phys. Rev. Lett.* **86**(17), 3755 (2001).
- [16] A. Dorn, A. Kheifets, C. D. Schröter, B. Najjari, C. Höhr, R. Moshhammer, and J. Ullrich, *Phys. Rev. A* **65**(3), 2709 (2002).
- [17] A. Lahmam-Bennani, A. Duguet, C. D. Cappello, H. Nebdi, and B. Piraux, *Phys. Rev. A* **67**(1), 0701 (2003).
- [18] A. Dorn, A. Kheifets, C. D. Schröter, C. Höhr, G. Sakhelashvili, R. Moshhammer, J. Loer, and J. Ullrich, *Phys. Rev. A* **58**, 012715 (2003).
- [19] D. Fischer, R. Moshhammer, A. Dorn, J. R. C. López-Urrutia, B. Feuerstein, C. Höhr, C. D. Schröter, S. Haggmann, H. Kollmus, R. Mann, et al., *Phys. Rev. Lett.* **90**, 243201 (2003).
- [20] C. Dupré, A. Lahmam-Bennani, A. Duguet, F. Mota-Furtado, P. F. O'Mahony, , and C. Dal-Cappello, *J. Phys. B* **25**, 259 (1992).

- [21] L. Avaldi, R. Camilloni, R. Multari, G. Stefani, J. Langlois, O. Robaux, R. J. Tweed, and G. N. Vien, *J. Phys. B* **31**, 2981 (1998).
- [22] A. S. Kheifets and K. Bartschat, in *23d International Conference on Photonic, Electronic and Atomic Collisions* (Stockholm, Sweden, 2003).
- [23] D. R. Bates, A. Fundaminsky, and H. S. W. Massey, *Philos. Trans. R. Soc. London, Ser. A* **243**, 13 (1950).
- [24] A. Franz and P. L. Altick, *J. Phys. B* **28**(21), 4639 (1995).
- [25] M. Abramowitz and I. A. Stegun, *Handbook of mathematical functions with formulas, graphs, and mathematical tables* (Academic Press, New York, 1975).
- [26] D. A. Varshalovich, *Quantum theory of angular momentum* (World Scientific Pub., Philadelphia, 1988), 1st ed.
- [27] Y. Fang and K. Bartschat, *Phys. Rev. A* **64**, 020701 (2001).
- [28] I. Taouil, A. Lahmam-Bennani, A. Duguet, M. Lecas, and L. Avaldi, *Phys. Rev. Lett.* **81**(21), 4600 (1998).
- [29] A. S. Kheifets and I. Bray, *Phys. Rev. A* **65**(1), 2710 (2002).
- [30] A. S. Kheifets, in *International Symposium on (e,2e), Double Photoionization and Related Topics* (Koenigsstein, Germany, 2003).
- [31] C. Plottke, I. Bray, D. Fursay, and A. Stelbovics, in *23d International Conference on Photonic, Electronic and Atomic Collisions* (Stockholm, Sweden, 2003).